Supporting Information

SI Material and Methods

Patient's selection and colonic biopsies collection

The present study includes fresh colonic biopsies obtained from 75 patients (including 3 patients in remission stage) diagnosed with UC that underwent scheduled colonoscopy (between 2014 and 2017) at the Gastroenterology Department of Centro Hospitalar do Porto- Hospital de Santo António (CHP-HSA), Porto, Portugal. Fresh colonic biopsies (5-10 biopsies per patient) were representative of macroscopically active disease topography, as defined by Mayo endoscopic score (41) and intestinal $CD3^+$ T cells were purified. Blood was also collected for T cell isolation at the time of colonoscopy.

The eligibility criteria for inclusion in this study were UC patients with inaugural disease (naïve, without therapy) or with standard 5ASA therapy with no history of human immunodeficiency virus infection or cancer.

Normal controls (n=3) are represented by individuals that attend the gastroenterology department of CHP-HSA for a planned colonoscopy (no history of IBD or cancer).

All specimens were subjected to histological examination and classification. All participants gave informed consent about all clinical procedures and research protocols were approved by the ethics committee of CHP/HSA, Portugal (233/12(179- DEFI/177-CES).

Isolation of $CD3^+$ T cells from fresh colonic biopsies and blood of active UC patients. *Ex vivo* culture of T cells.

Colonic biopsies from controls, inactive and active UC patients were mechanically dissociated to prepare single cell suspensions using the Hanks' Balanced Salt solution Modified medium, without calcium chloride and magnesium sulfate (HBSS) (Sigma) with Penicilin/Streptomycin and Gentamicin. Peripheral Blood Mononuclear Cells (PBMCs) were obtained by density gradient centrifugation using Lymphoprep.

$CD3^+$ T cells (from biopsies and blood) were magnetically sorted by using the EasySep™ Human T Cell Enrichment Kit (STEMCELL) following the manufacturer's instructions. $CD3^+$ T cells (2×10^4) were cultured for 72h in 96-well round bottom plates with plate-bound anti-CD3 mAb (clone OKT3) (0,5μg/ml) and soluble anti-CD28 (clone CD28.2) mAb (0,5μg/ml) (eBioscience). *N*-acetylglucosamine (GlcNAc) (Sigma and Wellesley Therapeutics Inc) was added to the T cells cultures (0, 40, 80, 100mM). Kifunensine (10μm) and Swainsonine (500nM) (both from Sigma) were used as inhibitors of N-glycosylation, specifically inhibits the enzymes mannosidase I (α-MAN I) and mannosidase II (α-MAN II), respectively (Supplementary Fig.1a). D-Mannose (80, 100 mM) (Sigma).

Imaging Flow Cytometry

Imaging flow cytometry analysis was performed as previously described (42) to assess co-localization of the $TCR\alpha/\beta^+$ with L-PHA on T cells cultured for 72h under T cell-stimulation and different concentrations of GlcNAc. Data acquisition was performed in ImageStreamX (Amnis, Millipore). Data analysis was performed using IDEAS 5.0 software (Amnis, EMD Millipore), to determine the percentage of TCR^+

cells, mean bright detail similarity and mean fluorescence intensity of L-PHA at the cell membrane by creating a specific mask to evaluate fluorescence at the cell membrane.

Flow cytometry

$CD3^+$ T cells were resuspended in PBS containing 10mM sodium azide and 2%BSA and incubated for 30 min at 4°C with specific conjugated antibodies (detailed Table S1) and for β1,6-GlcNAc branched N-glycans detection, fluorescein isothiocyanate (FITC)-conjugated L-PHA (Vector Lab) (2µg/ml). Results were expressed as percentage (%) of cells that stained positively for CD4 and CD8, as well as the MFI due to L-PHA staining within each T cell population.

For cell surface and intracellular antigens used are indicated in TableS1. Surface-stained cells were fixed and permeabilized using the Foxp3/Transcription Factor Staining Buffer Set (eBioscience) according to manufacturer's instructions. Fluorescence minus one stainings and isotype controls (eBioscience) were included for each assessed transcription factor.

For cytokine intracellular staining, $CD3^+$ T cells, cultured as described above for 72 h with anti-CD3 and anti-CD28, were washed with fresh medium and further incubated for 3 h at 37 °C in complete RPMI medium containing 500 ng/mL of ionomycin, 50 ng/mL PMA and 10 µg/mL of Brefeldin A (all from Sigma). Cells were stained with APC-eFluor® 780 Fixable viability dye before being surface stained with PerCP Cy 5.5 anti-human CD4 (clone RPA-T4) (Biolegend). Cells were then fixed with 2% formaldehyde, washed, permeabilized with 0.5% saponin (Sigma) and pre-incubated with 2% mouse serum before intracellular staining with human antibodies for TNF-α and IFN-γ (details in Table S1) or respective isotype controls (all from eBioscience).

In all flow cytometry experiments, dead cells were excluded with Fixable Viability Dye APC-eFluor® 780-conjugated (eBioscience).

Data acquisition was performed on a FACSCanto™ II system (BD Biosciences, San Jose, CA) using the FACSDiva™ software (BD) and compensated and analysed in FlowJo version 10.4. (Tree Star, Inc., Ashland, OR). Doublets were excluded from the analysis based on FSC-A versus FSC-H parameters. Fluorescence minus one gating was used to define the gates for cytokine-producing cells. Isotype controls were used to evaluate unspecific staining.

Proliferation assay

For T cell proliferation assays, $CD3^+$ cells were purified from colonic biopsies of naïve patients (with inaugural disease) and 5-(and-6)- carboxyfluorescein diacetate succinimidyl ester (CFSE)-labelled using the CellTrace CFSE Cell Proliferation Kit (Molecular Probes, Invitrogen), as previously described (43), prior to culture. Dead cells were excluded based on propidium iodide incorporation. Acquisition was performed in an EPICS XL cytometer (Beckman-Coulter Corporation) and data were analyzed (always gating in live cells) using FlowJo software.

Cytokine production

Supernatants from colonic T cell cultures (treated and untreated) were analyzed by flow cytometry using the BD™ Cytometric Bead Array (CBA) Human Th1/Th2/Th17 Cytokine Kit (BD) following the manufacturer's instructions. Sample acquisition was performed in BD FACS Canto^{TM} II flow cytometer (Becton Dickinson) and data were analyzed using the Flow Cytometric Analysis Program (FCAP) Array^{TM}

software. Human TGF-β1 was quantified in the concentrated culture supernatants by using the ELISA kits (R&D systems), according to manufacturer's instructions.

The supernatants from mouse colonic explant cultures were concentrated 15 fold by using Amicon® Ultra-2 mL Centrifugal Filters (Merck Millipore, Billerica, MA), according to manufacturer's instructions. The levels of the cytokines IFN-γ and IL-17A were quantified in the concentrated culture supernatants by using the respective anti-mouse Ready-Set-Go!® ELISA kits (eBioscience), according to manufacturer's instructions. The levels of the cytokines TNF-α and IL-6 were quantified in the concentrated culture supernatants by using the respective anti-mouse (Biolegend), according to manufacturer's instructions.

Western-blot and TCR signaling

TCR signaling was evaluated by assessing the phosphorylation levels of LAT and ZAP70. After 72h of *ex vivo* T cell culture in absence or presence of GlcNAc lysates were extracted using RIPA buffer. Twenty µg of protein lysates were separated by 12% SDS–PAGE electrophoresis and transferred onto nitrocellulose membranes (GE Healthcare, Life Sciences, UK). Membranes were blocked before incubation phospho-Zap-70 (Tyr319/Syk (Tyr352) rabbit mAb (1:500) and anti-phospho-LAT (Tyr191) rabbit mAb (1:500) (both from Cell Signaling Technologies, USA). Goat anti-rabbit IgG-HRP mAb (Santa Cruz Biotechnology, USA) was used as secondary antibody.

For L-PHA lectin blot analysis (44), 20µg of T cell protein lysates separated by 12% SDS-PAGE electrophoresis was performed as in previous methods(16) . For loading control analysis, mouse IgG anti-tubulin (Sigma) or rabbit IgG anti-actin (Santa Cruz Biotechnology,USA) was used. The target proteins were visualized using ECL reagent (GE Healthcare, Life Sciences). Positive reaction was observed in a band the

same size as TCRβ (mouse monoclonal antibody anti-human, Santa Cruz Biotechnology, USA) (39kDa, accordingly with manufacturer antibody details).

Immunoprecipitation

For T cell receptor (TCR) immunoprecipitation (IP), equal amounts of total cell lysates (TCL) obtained from mouse colons or from *ex vivo* human T cell cultures (in absence or presence of GlcNAc) were treated as previously described(16). Positive reaction was observed in a band the same size as rabbit anti-human TCR β (39kDa) polyclonal antibody (Santa Cruz Biotechnology).

Glycophenotype

T cells were incubated with biotinylated L-PHA (2µg/ml), biotinylated LEL (recognizes poly-lactosamine structures) (1 µg/ml), biotinylated SNA (recognizes α2,6 sialic acid) (5µg/ml) or biotinylated MALII (recognizes α2,3 sialic acid) (10µg/ml) (Vector Labs, USA). Lectins were revealed with (FITC)-conjugated streptavidin. FITC-conjugated streptavidin alone was used as control. Propidium iodide (PI) was used to exclude dead cells. Data acquisition was performed in a FACS Canto™ II flow cytometer. Data were analyzed using FlowJo software.

Apoptosis assays

Apoptotic cells were identified by flow cytometry using the FITC Annexin V Apoptosis Detection Kit I (BD Biosciences), following the manufacturer's instructions. Only cells staining positive with FITC-Annexin V and negative with propidium iodide

(indicative of early apoptosis) were considered. Data acquisition was performed in a FACS Canto™ II flow cytometer. Data were analyzed using FlowJo software.

Enzymatic reaction and HPLC analysis

Blood and colonic T cells of UC patients and controls were prepared as described above to evaluate the enzymatic activity of GnT-V, using a previously described methodology (45).

DSS and TNBS-induced colitis and *in vivo* GlcNAc treatment

Intestinal inflammation was induced in both male and female C57BL/6 mice, MGAT5 wildtype (WT), heterozygous (*MGAT5*$^{+/-}$), knockout mice (*MGAT5*$^{-/-}$) (kindly provided by Prof. Michael Pierce, CCRC, Georgia University, Athens, USA) , (6 to 8 weeks old), at IPATIMUP/i3S's animal facility by treating *ad libitum* with 2% dextran sodium sulfate (DSS) (36,000–50,000 Da; MP Biomedicals) in the drinking water, as previously described (19). The 2,4,6-trinitrobenzene sulfonic acid (TNBS) model was also performed using male C57BL/6 mice (6 to 8 weeks old), following previously described protocols(19) and including the following groups (animals randomly distributed): Control Group_water (H_2O, via rectal), Control Group_ethanol (50% ethanol, via rectal) and Group TNBS (3% TNBS in 50% ethanol, via rectal).

All procedures involving animals and their care were conducted in conformity with institutional guidelines in compliance with national and International laws and policies on the protection of animals used for scientific purposes (Directive 2010/63/EU, Guide for the Care and Use of Laboratory Animal. Eight edition, 2011). All the procedures were approved by local and national committees.

Both colitis models showed a dysregulation of branched N-glycosylation on T cells in mice with colitis (Supplementary Fig. 8a-b). In this study we have chosen the DSS model of colitis because it does not interfere with the enema treatment strategy the as TNBS model, that imply a rectal induction, would originate biased results.

The therapeutic effects of GlcNAc administration were evaluated by treating the DSS mice with GlcNAc (Sigma and Wellesley Therapeutics Inc) after disease onset, either orally by supplementing the drinking water at 0.25 mg/ml (as previously described (12)) and/or rectally, by GlcNAc enemas at 0.5 mg/ml (using a catheter). Treatment was performed daily for 7 consecutive days (19).Animals were randomly distributed per group of treatment. Oral consumption was verified by measuring the amount of drinking water left over each treatment.

Mice were clinically evaluated daily and over the next 7 days upon GlcNAc treatment and scored in a blinded fashion as follows: body weight change (values of body weight are expressed as percentage of body weight on day 0) ; disease activity index (DAI), the mean of the following parameters: % weight; stool consistency and blood stool (46).

The evaluation of colitis onset and disease severity in mice with different *MGAT5* genotypes: C57BL/6 wild-type mice (n=14); *MGAT5*$^{+/-}$ (n=23) and *MGAT5*$^{-/-}$ (n=11) was based on DAI score per animal per day. Active disease was defined when animals showed DAI $\geq$ 2 and three stages of severity were defined: mild ($\geq$2 and < 2,5), moderate ($\geq$2,5 and <3) and severe ($\geq$3).

In both *in vivo* models (TNBS and DSS), lamina propria T lymphocytes (LPLs) were isolated from mice colon samples following previously described methods (16).

Tissue immunohistochemistry and immunofluorescence

Formalin-fixed paraffin-embedded (FFPE) colonic tissue slides prepared from the different group of animals were used for H&E staining to evaluate histopathological alterations, and for immunohistochemistry with L-PHA and anti-CD3 mAb, following a previously described protocol(16). The evaluation of the mucus layer was focused on glycoproteins and glycans modifications in proteins (such as TCR) not removed by FFPE processing(47). Immunohistochemistry to evaluate Foxp3 and F4/80 expression was evaluated as described in (48).

T-bet immunofluorescence, in colon sections, was performed using heat-induced antigen retrieval with EDTA (Sigma), blocking with goat normal serum (Dako, diluted) before incubation with mouse IgG_1 T-bet-specific mAb (clone 4B10, Santa Cruz, 1:50) overnight, at 4ºC. Then slides were incubated with goat anti-mouse Alexa 594 secondary antibody (Invitrogen, 1:250) following nuclear staining with DAPI (1:100). Immunofluorescent images were obtained using a Zeiss Imager.Z1 AxioCam MRm (Carl Zeiss).

Real -time PCR

Total RNA from isolated LPLs was extracted and the quantitative real-time PCR (qRT-PCR) was performed using TaqMan Gene Expression Assays (Applied Biosystems) as previously described (16). qRT-PCR was carried out in triplicates using RNA source from intestinal LPLs from MGAT5 null mice controls (n=2) versus GlcNAc treated mice after DSS (n=2), for the target gene MGAT5b (Taqman probe: Mm01252571_m1, Applied Biosystems) and for the appropriated lymphocytes endogenous control 18S (Hs99999901_s1, Applied Biosystems).

Statistical analysis

Statistical significance was assessed by one-way or two-way analysis of variance (ANOVA) using Bonferroni's, Dunnett's or Newman–Keuls multiple comparison post-tests and, where appropriate, by unpaired Student's t-test (two-tailed) using GraphPad Prism 5. *P* values of <0.05 were considered statistically significant.

In the *in vivo* studies, we have estimated the number of animals per genotype n >20, α= 0,05 and power >0,07. Statistical outliers were identified and excluded from the analysis, such as the animals that were euthanized when they reached the established humane endpoints.

SI Appendix Fig. S1

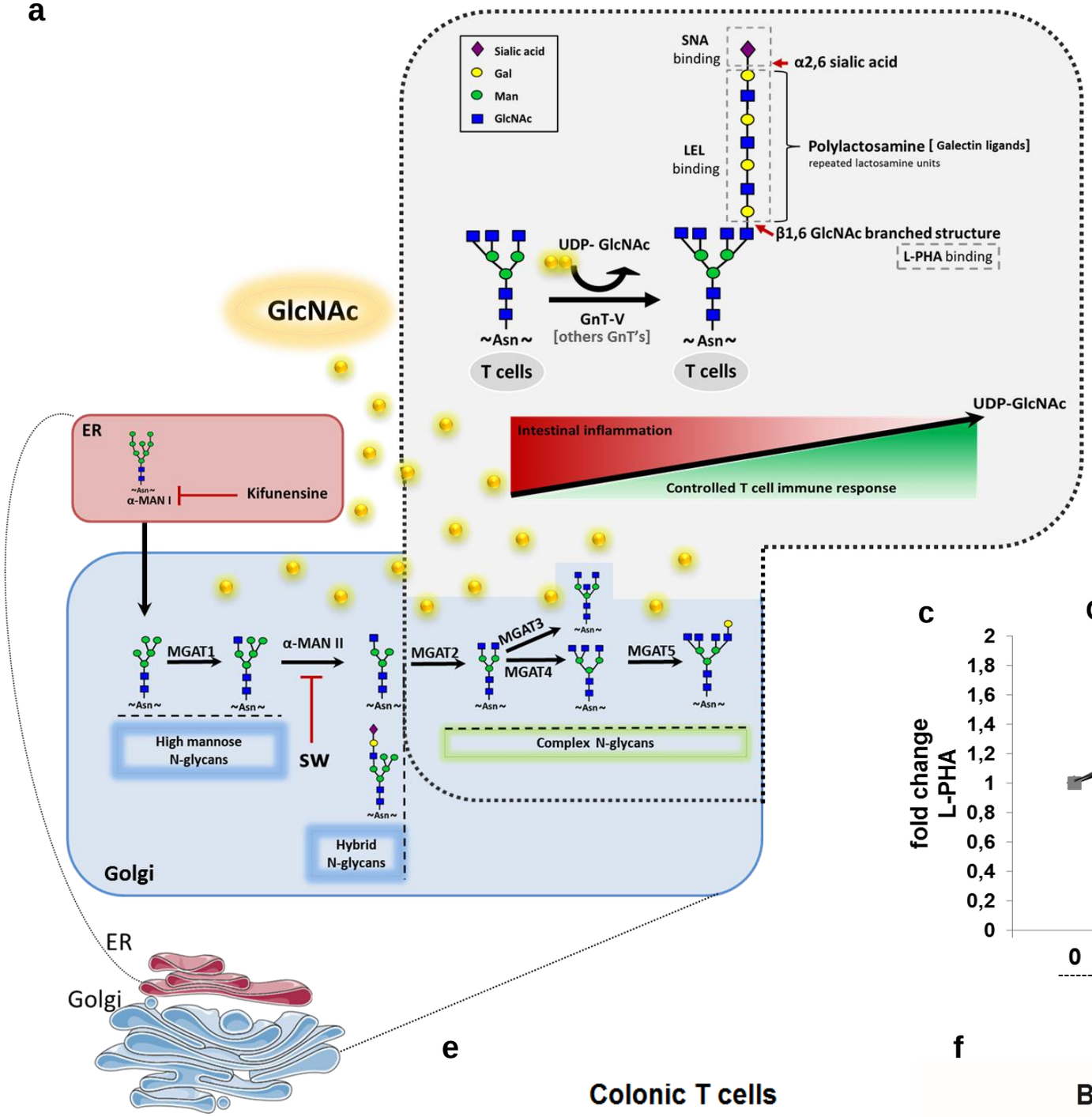

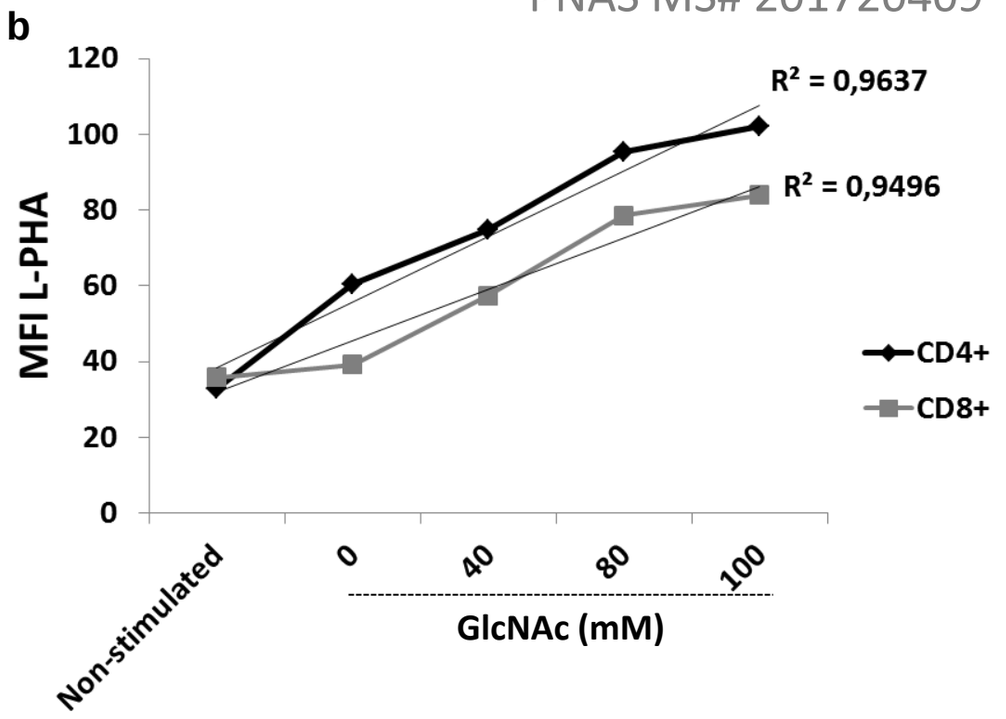

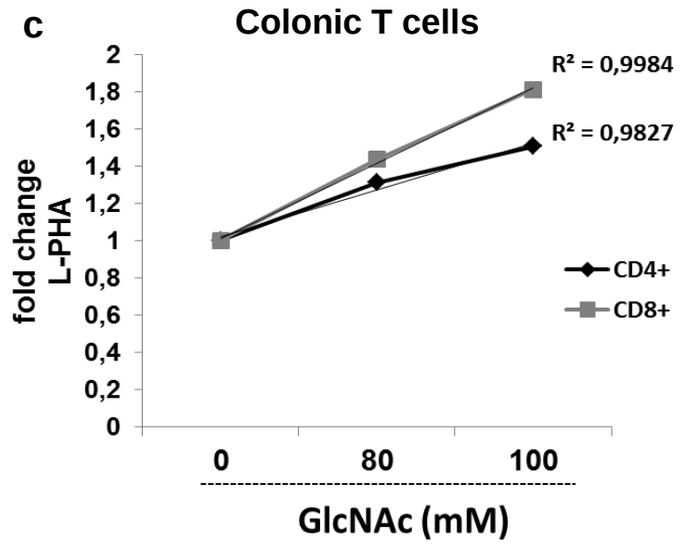

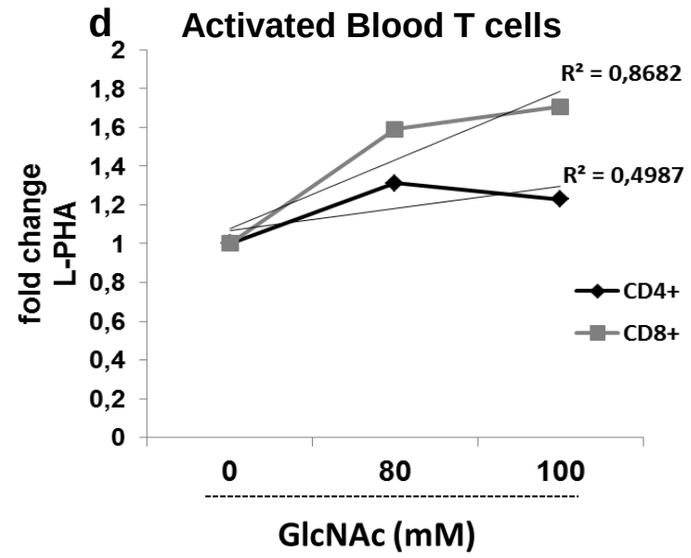

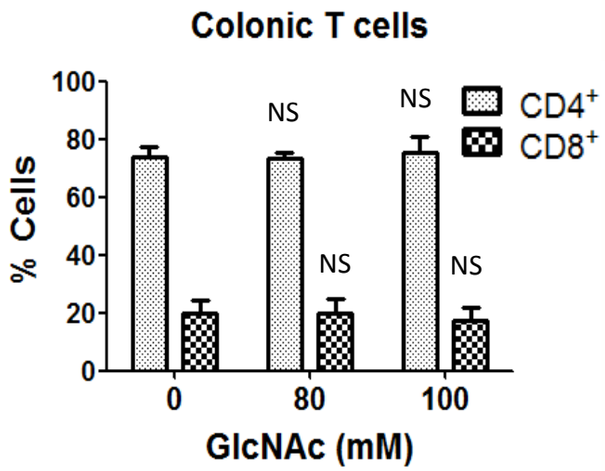

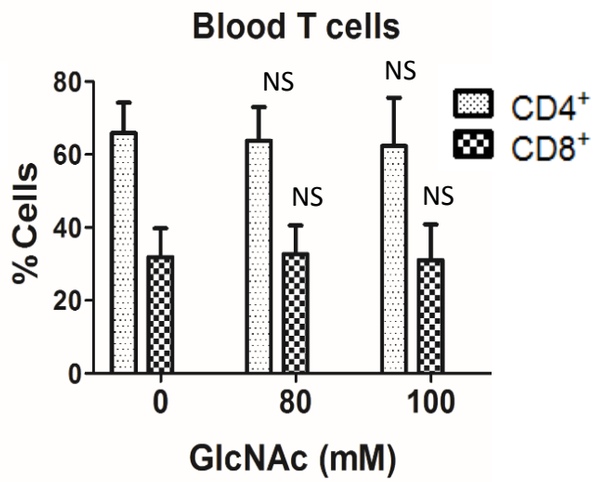

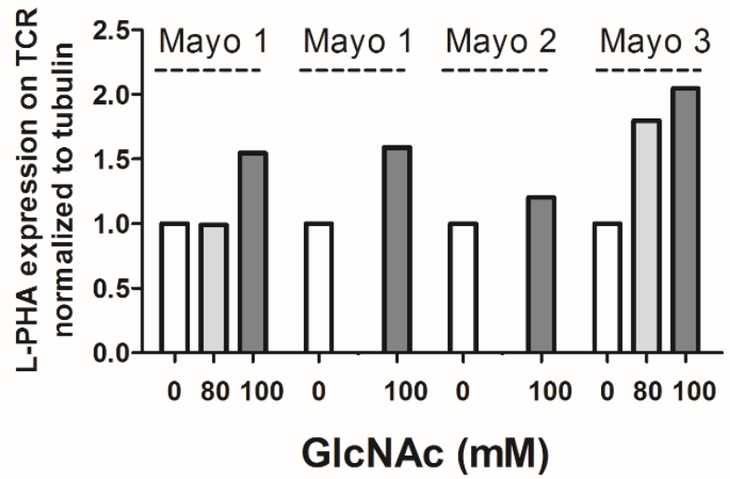

SI Appendix Fig. S2

PNAS MS# 201720409

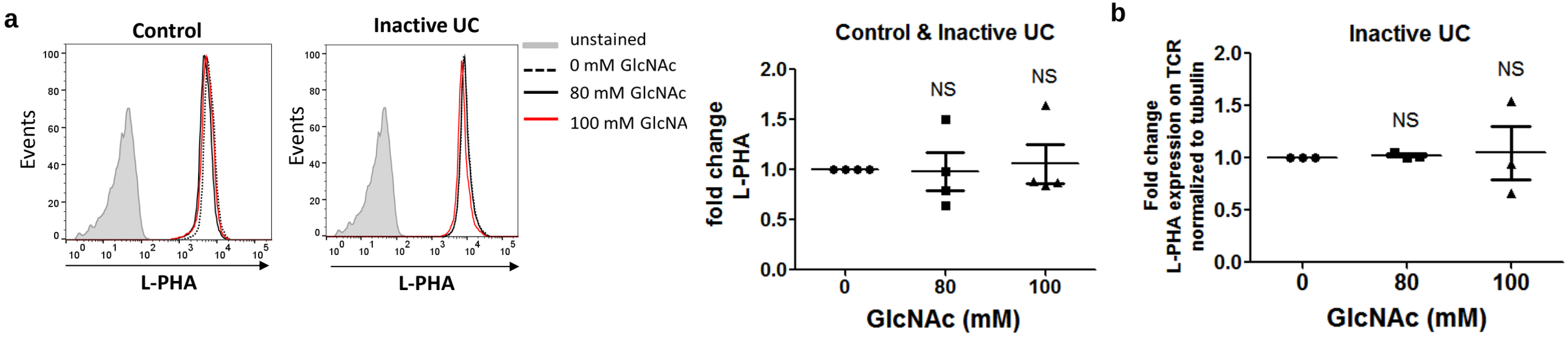

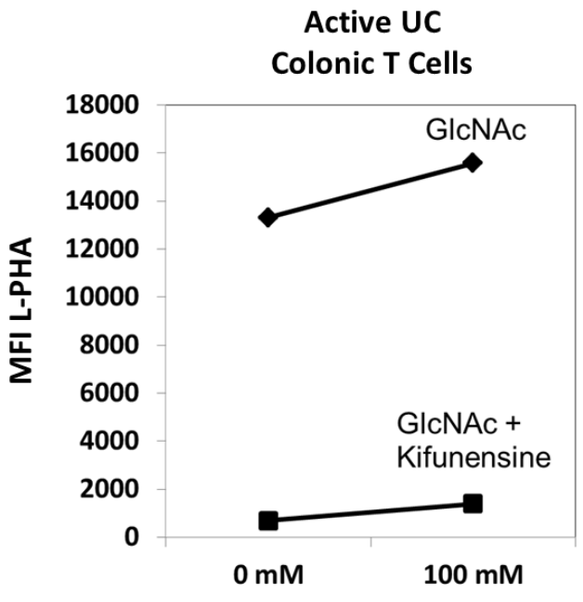
Active UC
Colonic T Cells
MFI L-PHA
18000
16000
14000
12000
10000
8000
6000
4000
2000
0
GlcNAc
GlcNAc +
Kifunensine
0 mM
100 mM

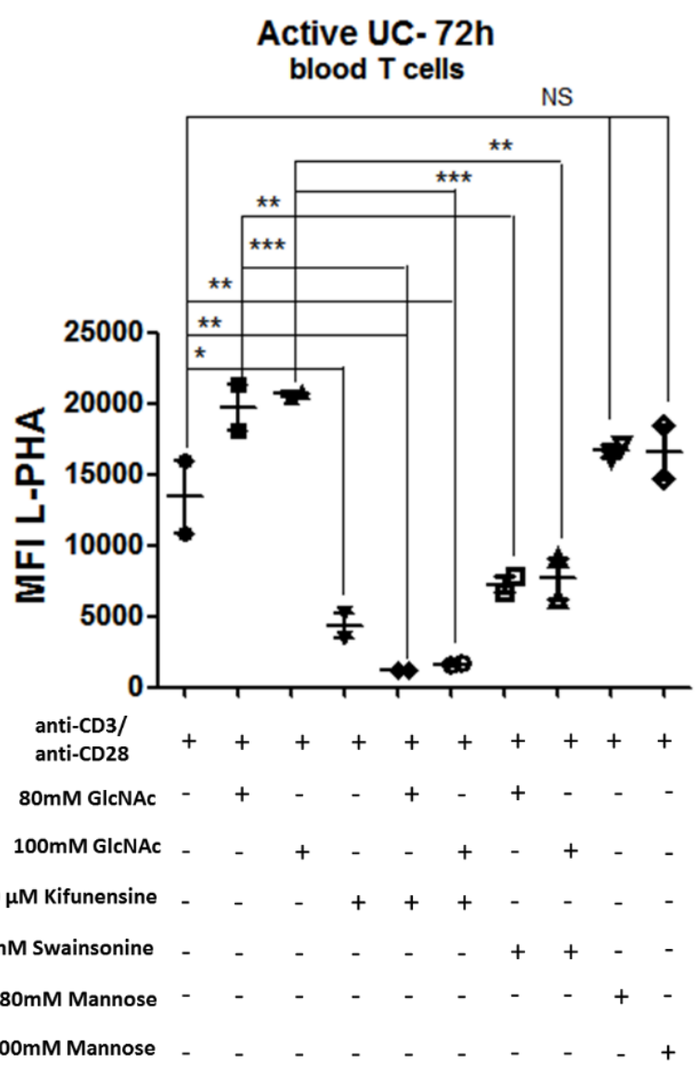
Active UC- 72h
blood T cells
MFI L-PHA
25000
20000
15000
10000
5000
0
NS
**
***
**
***
**
**
*
anti-CD3/
anti-CD28
80mM GlcNAc
100mM GlcNAc
10 µM Kifunensine
500 nM Swainsonine
80mM Mannose
100mM Mannose

SI Appendix Fig. S4

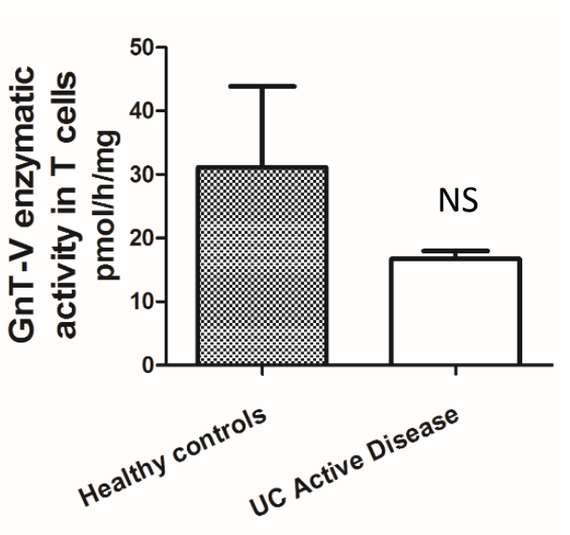

PNAS MS# 201720409

a

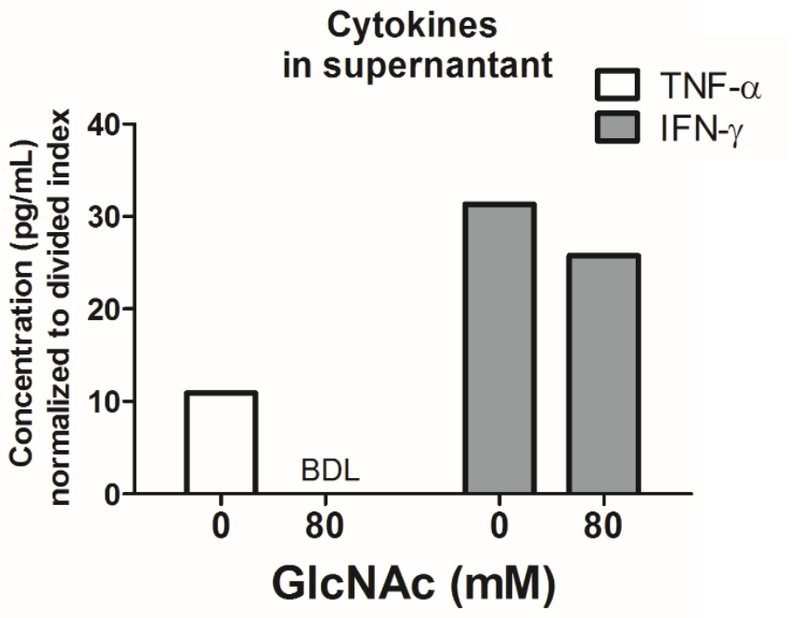

b

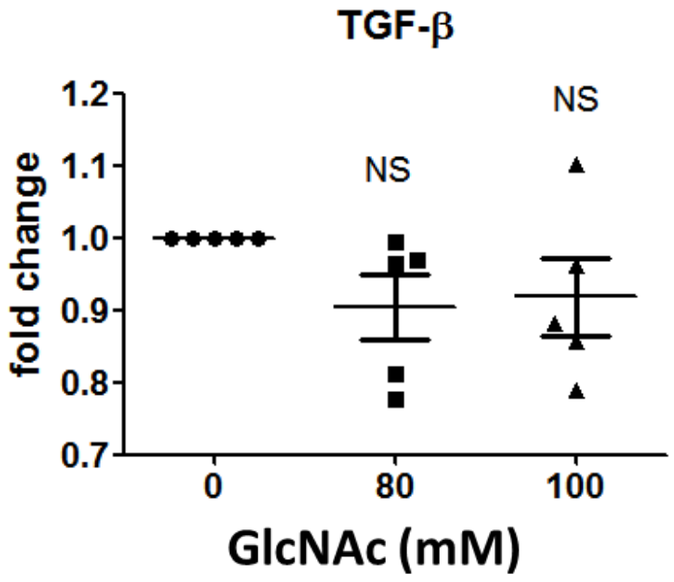

c

	IL-10 secreted by Active UC colonic T cells (pg/ml)		
	0 mM	**80 mM GlcNAc**	**100 mM GlcNAc**
Patient 1	15,24	11,1	4,87
Patient 2	0,28	0	0
Patient 3	7,8	4,57	3,02
Patient 4	0	0	0
Patient 5	0,38	0	0
Patient 6	1,5	0,61	0,35

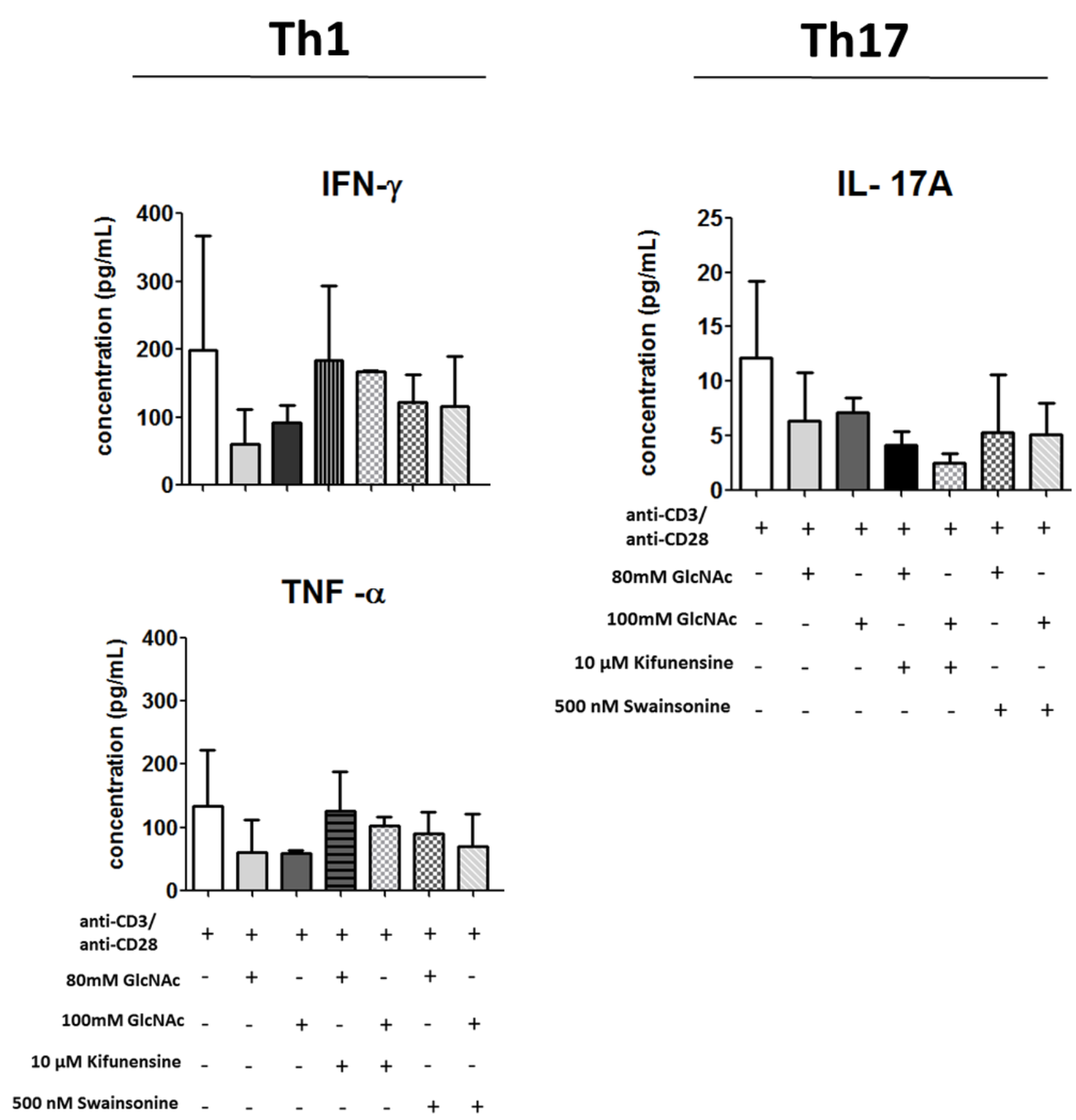
Th1
Th17
IFN-γ
IL- 17A
TNF -α
concentration (pg/mL)
400
300
200
100
0
25
20
15
10
5
anti-CD3/
anti-CD28
80mM GlcNAc
100mM GlcNAc
10 µM Kifunensine
500 nM Swainsonine
+
-

PNAS MS# 201720409

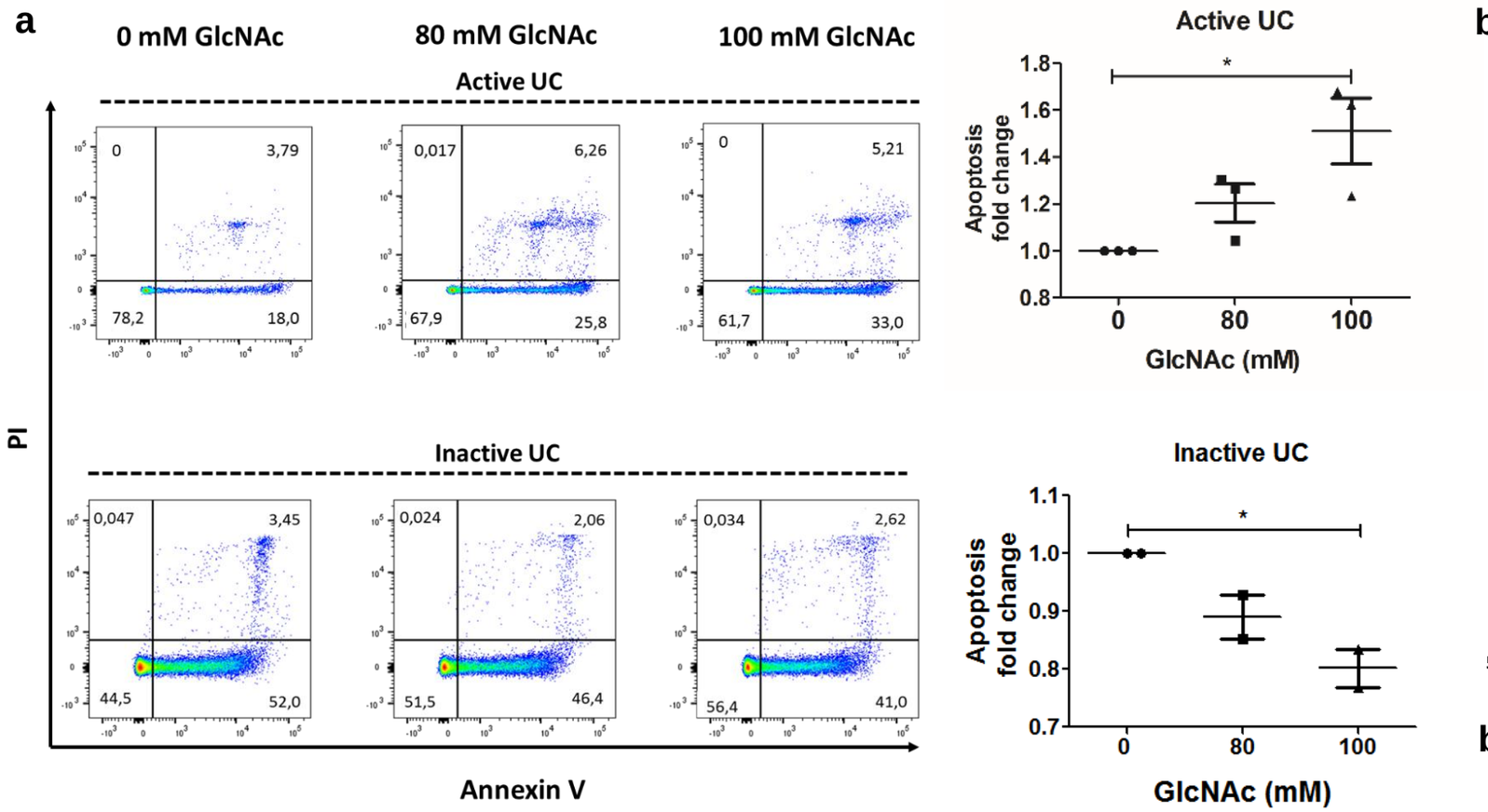

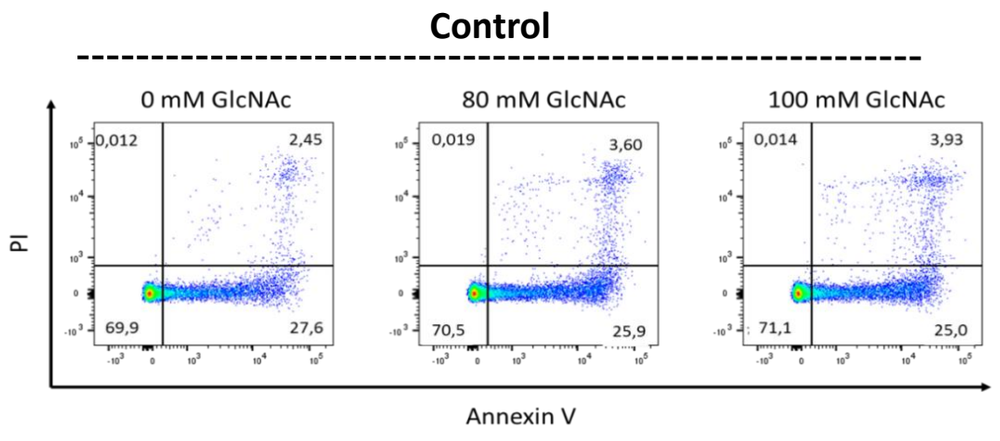

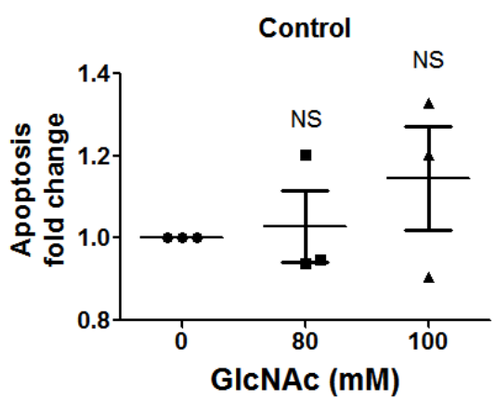

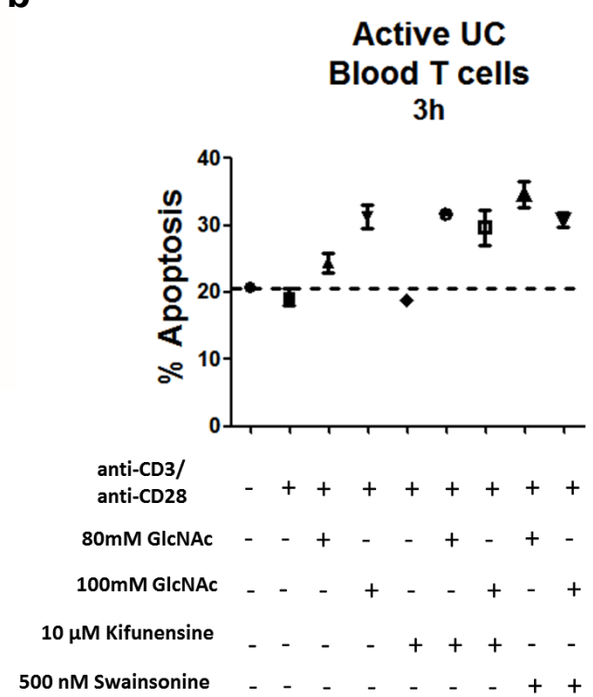

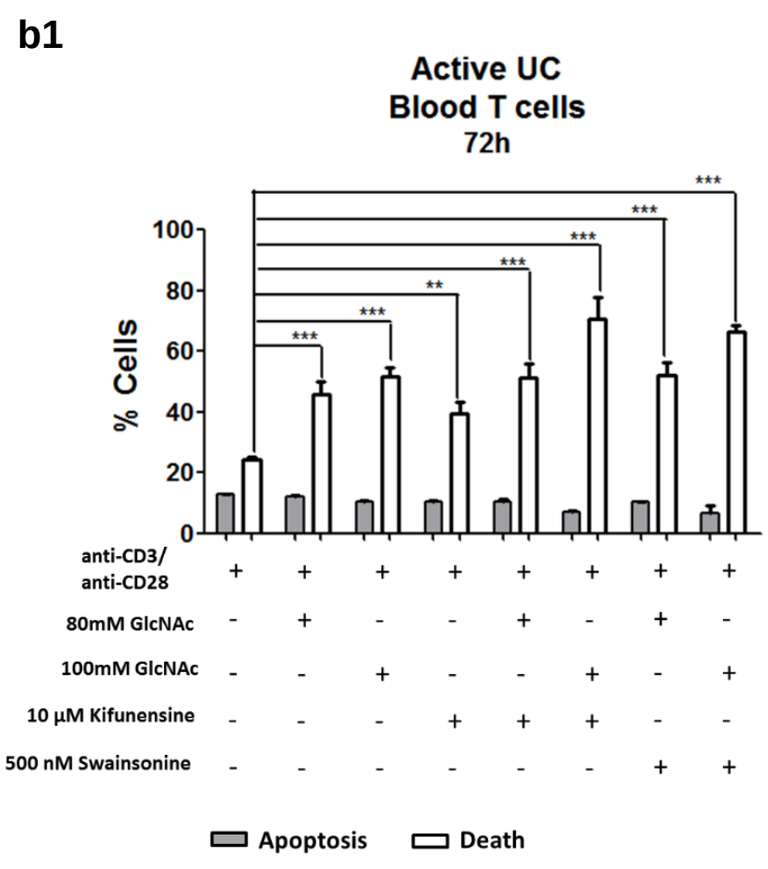

PNAS MS# 201720409

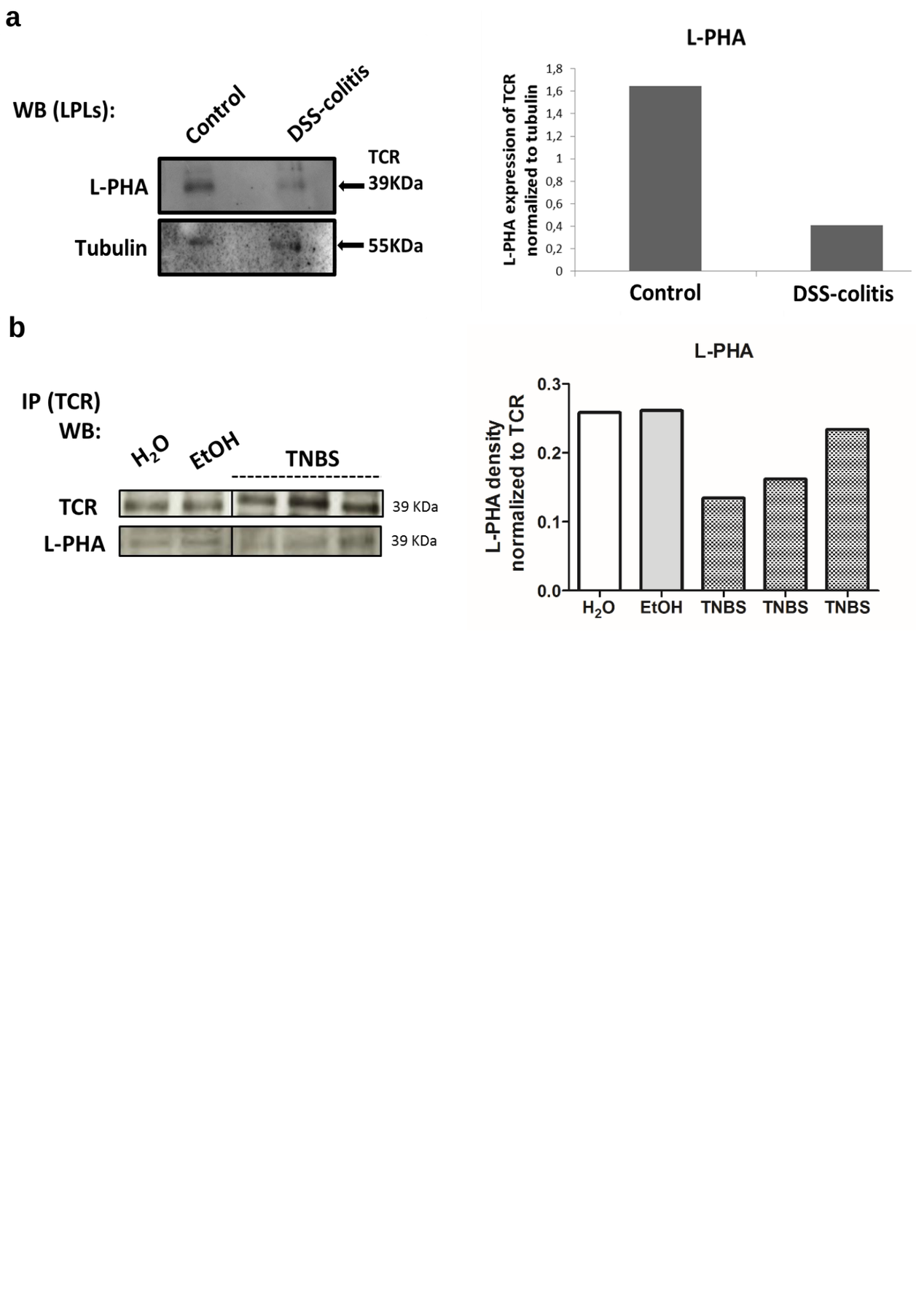

PNAS MS# 201720409

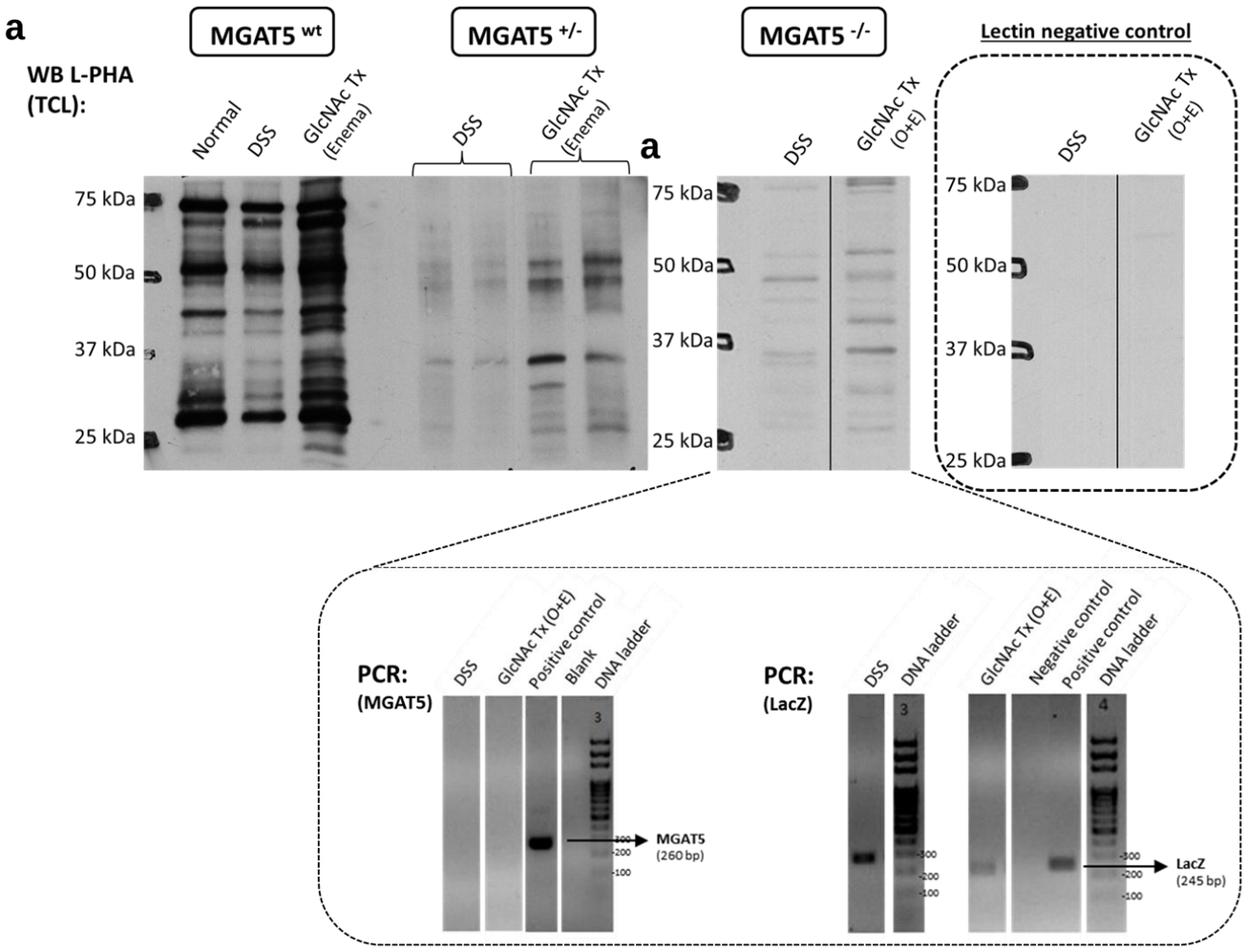

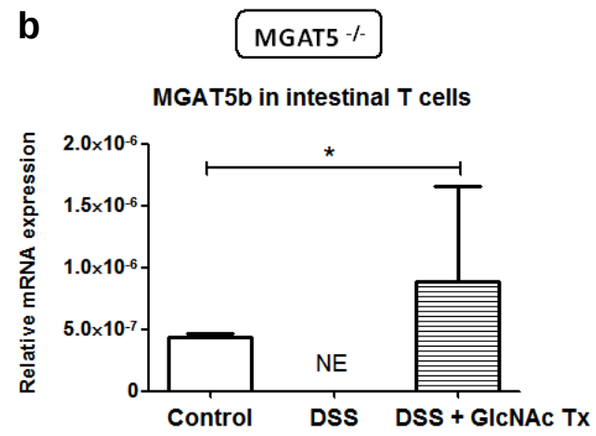

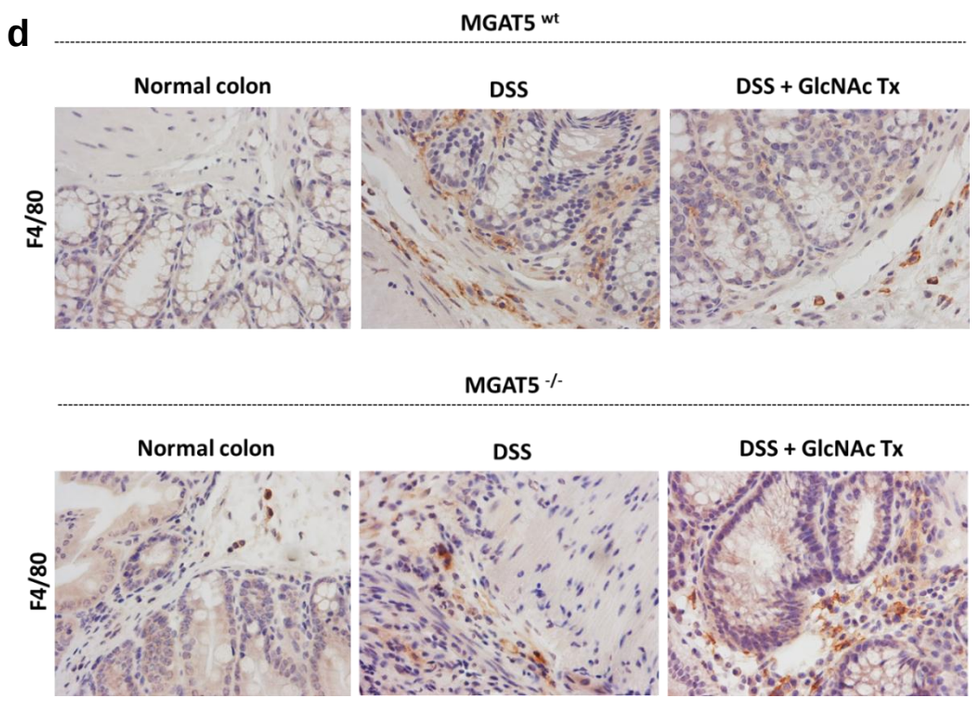

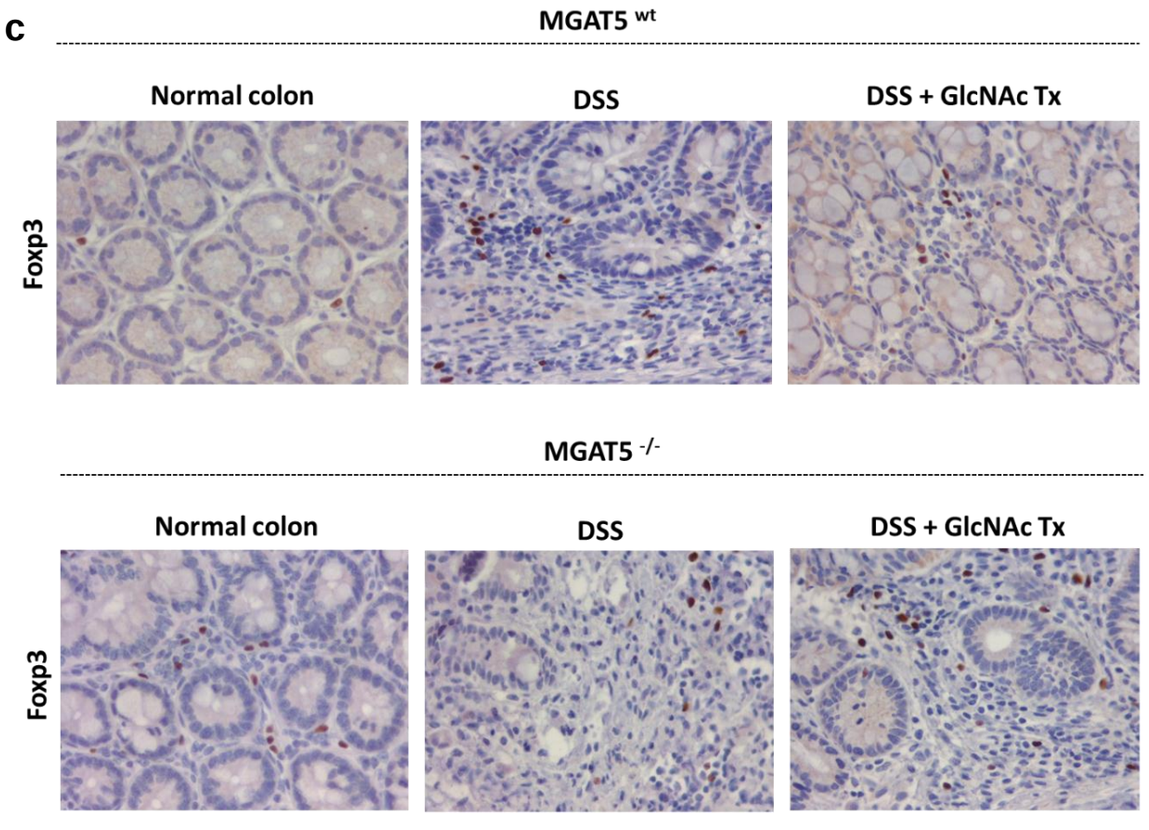

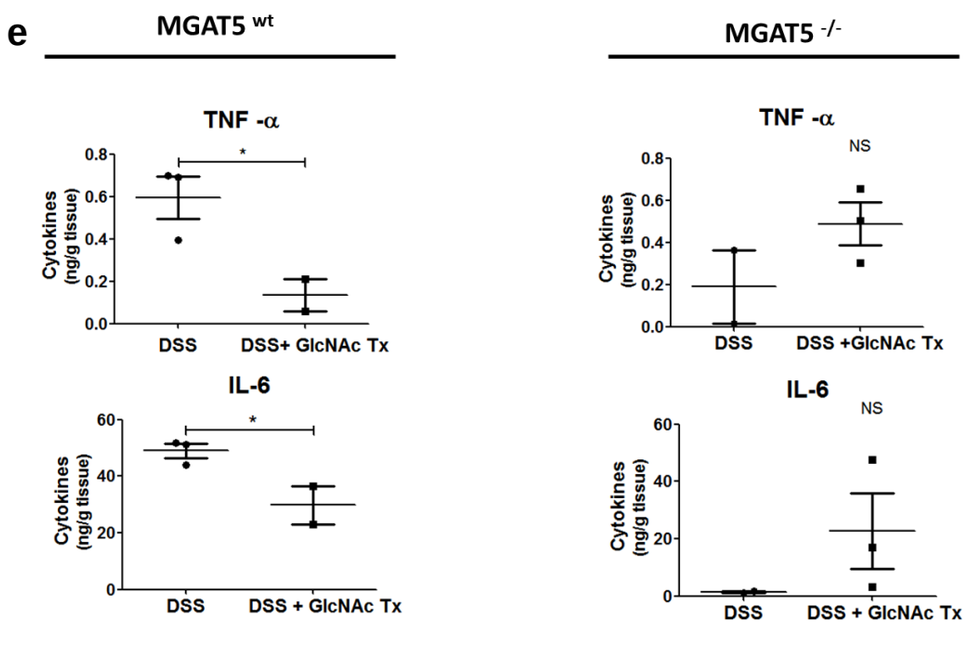

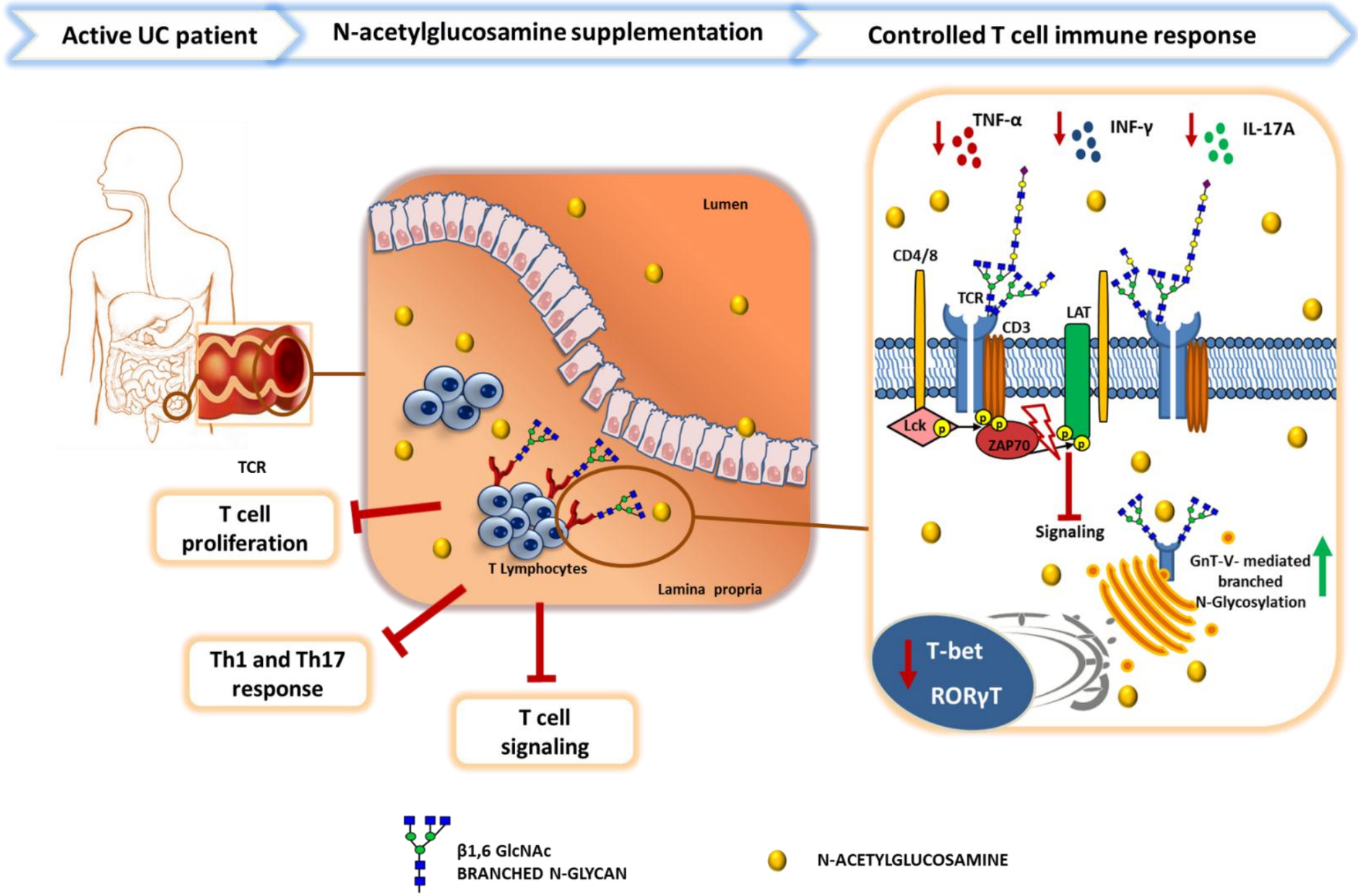
Active UC patient
N-acetylglucosamine supplementation
Controlled T cell immune response
TCR
T cell proliferation
Th1 and Th17 response
T cell signaling
Lumen
T Lymphocytes
Lamina propria
TNF-α
INF-γ
IL-17A
CD4/8
TCR
CD3
LAT
Lck
ZAP70
Signaling
GnT-V- mediated branched N-Glycosylation
T-bet
RORγT
β1,6 GlcNAc BRANCHED N-GLYCAN
N-ACETYLGLUCOSAMINE

Supporting Information

SI figure legends

Fig. S1. Enhancing *ex vivo* the hexosamine biosynthetic pathway in T cells by metabolic supplementation with N-acetylglucosamine (GlcNAc). (**a**) Schematic representation of T cells glycophenotype upon GlcNAc supplementation. In the canonical pathway, the GnT-V glycosyltransferase catalyzes the addition of β1,6-GlcNAc branched N-glycans (as detected by L-PHA lectin) on T cells that are further extended with polylactosamine structures (detected by plant lectin *Lycopersicon esculentum* agglutinin (LEL)). Additionally, our results demonstrate a trend increase in α2,6- linked sialic acid recognized by binding of *Sambucus nigra* agglutinin (SNA) and no significant alteration in α2,3- sialic acid residues. This glycosylation signature in T cells was shown to regulate the adaptive immune response. (**b**) $CD3^+$ T cells, magnetically sorted from blood of active UC patient were cultured for 72h under anti-CD3/CD28 mAb stimulation. Different concentrations (mM) of GlcNAc were added to cultures, as indicated. Fold change of L-PHA staining was determined by flow cytometry. (**c** and **d**) In $CD4^+$ and $CD8^+$ T cell subsets, N-glycosylation was determined by co-staining with L-PHA (lectin that recognize β1,6-branched N-glycans) and evaluated by flow cytometry. Fold change of L-PHA staining of $CD4^+$ and $CD8^+$ T cells sorted from intestinal biopsies or from blood of UC patients were *ex vivo* cultured for 72h under anti-CD3/CD28 mAb stimulation, in the presence of GlcNAc at indicated concentrations. (**e** and **f**) GlcNAc treatment does not affect the proportion of the T cell subsets. Results are presented as mean ± SEM of two to four independent experiments. (**g**) Fold change of L-PHA expression on a protein band corresponding to TCRβ migration profile normalized to tubulin. Results represent 4 biological replicates, using

T cells from patients at different stages of disease severity (Mayo 1 (n=2), Mayo 2 (n=1) and Mayo 3 (n=1)). Results are normalized to untreated that was taken as 1.

Fig. S2. Upon GlcNAc treatment, N-glycosylation of T cells from controls and UC inactive disease remains unaltered. (**a**) T cell N-glycosylation was determined by staining with L-PHA (lectin that recognize β1,6-branched N-glycans) and evaluated by flow cytometry. Fold change of L-PHA staining on *ex vivo* T cells from UC activated blood T cells after GlcNAc supplementation. Results of healthy controls (n=3) and UC inactive disease (n=2) are presented as fold change of MFI values ± SEM. (**b**) Protein lysates from the *ex vivo* colonic T cells from inactive UC patients (n=3), after supplementation with GlcNAc, were subjected to L-PHA lectin blot in order to evaluate the expression levels of β1,6-GlcNAc branched N-glycans on a protein band with the size of the TCRβ. Quantification of L-PHA densities on TCRβ band normalized to tubulin, presented as fold change relative to the 0 mM Glc condition. No significant alterations were observed in the expression of β1,6-GlcNAc branched N-glycans in T cells from inactive UC patients.

Fig. S3. Enhancement of branched glycosylation on T cells from active UC patients is abolished by specific inhibitors of branching N-glycans synthesis. Graphs represent the effect of the treatment of T cells isolated from biopsies (n=1, left) and blood (n=2, right) of active UC patients with GlcNAc and the inhibitors of branching N-glycans synthesis, Kifunensine and Swainsonine as well as a different sugar, D-mannose.

Fig. S4. T cells from active UC patients display reduced GnT-V enzymatic activity comparing with healthy controls. (**a**) Evaluation of the enzymatic activity of GnT-V assessed in a pool of lysates from colonic T cells obtained from different healthy individuals (n=2) and different active UC patients (n=2) and analyzed in two independent technical replicates.

Fig. S5. Secreted cytokines in supernatants of *ex vivo* T cells from active UC patients. (**a**) Concentration of pro-inflammatory cytokines detected in the supernatants from *ex vivo* cultures of mucosal T cells, normalized to respective division index (obtained from CFSE analysis) of T cells in the respective conditions (0 and 80 mM GlcNAc); BDL, means below detection limit. The effects of GlcNAc in the suppression of pro-inflammatory cytokines were found to be independent of cell death and/or decreased T cell proliferation. (**b**) Quantification of TGF-β in supernatants from *ex vivo* T cell cultures under GlcNAc supplementation. Scatter plots including mean fold change and ± SEM error bars of 5 biological replicates (biopsies: Mayo 2 (n=3); Mayo 3 (n=2). NS, not statistically significant. (**c**) The expression of IL-10 assessed by flow cytometry in supernatants from *ex vivo* T cell cultures under GlcNAc supplementation. Results include raw data of six biological replicates (Mayo 2 (n=3), Mayo 3 (n=3).

Fig. S6. Inhibition of branching N-glycans synthesis abrogates the regulation of pro-inflammatory cytokines production. Graphs represent the effect of *ex vivo* treatment of T cells isolated from blood (Mayo 3, n=1) of active UC patient with GlcNAc and the inhibitors of branching N-glycans synthesis, Kifunensine and

Swainsonine revealing no regulatory effects in T cell function, with no apparent impact in Th1- (TNF-α, IFN-γ) and Th17-associated (IL-17A) cytokine production.

Fig. S7. Impact of *ex vivo* GlcNAc treatment in cell apoptosis/death of T cells from control versus active UC patients. (**a**) Flow cytometry evaluation of T cell apoptosis by Annexin V/PI staining upon GlcNAc supplementation. The three dot plots correspond to a representative example of blood T cells from one active, one inactive UC patient and one heathy control. Numbers inside dot-plots correspond to the percentage of cells within each quadrant. Fold change in early apoptosis (Annexin V^+PI^-) after 3h of culture with and without GlcNAc, as indicated. Graphs correspond to mean fold change ± SEM of early apoptotic cells from biological replicates (Active: 3 biological replicates, Mayo 2 (n=2) and Mayo 3 (n=1); Inactive: 2 biological replicates; Control: 3 biological replicates). Results are normalized to the corresponding untreated condition that was taken as 1. Each value corresponds to the mean of two independent technical replicates. One-way ANOVA using Bonferroni's multiple comparison post-test: * $P \leq 0.05$. (**b**) Scatter plots correspond to percentages ± SEM of apoptotic cells at 3 hours in colonic T cells cultures from active UC patients, under different treatments and concentrations, as indicated. (**b1**) Percentage of apoptotic cells (Annexin V^+PI^-) and dead cells (Annexin V^+PI^+) in 72 hours cultures of blood T cells from active UC patients, under different treatments and concentrations, as indicated. Two-way ANOVA using Bonferroni's multiple comparison post-test: ** $P \leq 0.01$;*** $P \leq 0.001$.

Fig. S8. Evaluation of branched N-glycosylation on TCR of colonic T cells from DSS and TNBS-induced colitis mouse models. (**a**) Protein lysates from the isolated

colonic T cells from control mice (drinking water) and DSS-colitis mice (DSS in drinking water) were subjected to L-PHA lectin blot to evaluate the expression levels of β1,6-GlcNAc branched N-glycans on the TCRβ (39 kDa). Bar graph, quantification of L-PHA densities on TCR band normalized to tubulin. (**b**) Immunoprecipitation of TCR from total cell lysates of mouse colon followed by β1,6-GlcNAc branched N-glycans recognition with L-PHA as indicated. Bar in the graph correspond to the amounts of branched N-glycan structures, determined from the ratios of densities of L-PHA reactivity normalized to TCR, comparing control groups, water (H_2O, via rectum) and ethanol (50% ethanol, via rectum) with TNBS- induced colitis group (3% TNBS in 50% ethanol, via rectum). (**c**) Representative macroscopic images of the colon and cecum of *MGAT5* WT mice at the end of the experimental period: DSS control (DSS-induced colitis) and GlcNAc treatment (Tx) (DSS+ GlcNAc Tx, enemas), comparing with a normal colon. Mice under DSS treatment showed a visible colonic edema (swelling of the bowel wall) (arrowheads, further magnified in the inserts) comparing to normal mice or mice treated with GlcNAc (enemas route) after DSS-induced colitis.

Fig. S9. GlcNAc administration effects in different genotypes of MGAT5. (**a**) GlcNAc administration via enema reveal an enhancement of branched N-glycosylation on total cell lysates from mice with different MGAT5 genotypes. Evaluation of branching N-glycans on colonic total cell lysates from *MGAT5* ^{wt} mice, *MGAT5* $^{+/-}$ and *MGAT5* $^{-/-}$, comparing DSS control (DSS-induced colitis) with GlcNAc treatment Enema (GlcNAc Tx) by Western blot. Insert represents the *MGAT5* $^{-/-}$ genotyping (gels of PCR products of genes *MGAT5* and Lac Z) from the same animals represented in the *MGAT5* $^{-/-}$ L-PHA staining and lectin negative control. (**b**) Intestinal T cells from *MGAT5* null mice showed an increased expression of the homologous *MGAT5b* gene

upon GlcNAc treatment. qRT-PCR analysis for mRNA expression of MGAT5b from intestinal LPLs from MGAT5 null mice controls (n=2) *versus* GlcNAc treated mice after DSS (n=2), performed in triplicate. The mRNA expression levels are expressed as mean ± SEM, (Student's t-test: $*P \leq 0.05$). NE, not expressed. (**c**) T reg cells expression at the intestinal lamina propria of MGAT5 ^{wt} *versus* MGAT5 $^{-/-}$ mice. The impact on T reg cells was evaluated by the expression of Foxp3 by immunohistochemistry in the colon of MGAT5^{wt} mice and MGAT5 $^{-/-}$, comparing normal colon, DSS-induced colitis (DSS) and treated mice with GlcNAc (DSS + GlcNAc Tx). Represented colon sections of treated mice in both genotypes correspond to GlcNAc Oral+ Enema, x40 original magnification. (**d-e**) The control of inflammation upon GlcNAc treatment is associated with differences in *MGAT5* wildtype and null mice regarding macrophages recruitment and function. (**d)** The impact of GlcNAc treatment on macrophages was evaluated by the expression of F4/80 by immunohistochemistry in the colon of MGAT5^{wt} mice and MGAT5 $^{-/-}$, comparing normal colon, DSS-induced colitis (DSS) and treated mice with GlcNAc (DSS + GlcNAc Tx). Represented colon sections of treated mice in both genotypes correspond to GlcNAc Oral+ Enema, x40 original magnification. (**e**) Concentration of TNF-α and IL-6 in the supernatants of 24h colonic explant cultures from DSS and DSS + GlcNAc Tx *MGAT5* wildtype (n=5) and null (n=5) mice by ELISA. Cytokine levels are expressed as ng/g of dry colon explant weight. Results correspond to mean ± SEM of 2 to 3 animals per group. Student's t-test: $* P \leq 0.05$. NS, not statistically significant.

Fig. S10. Shaping the T cell-mediated immune response in IBD through metabolic enhancement of branched N-glycosylation. An opportunity for new therapeutic strategies. UC patients with active disease are characterized by a massive infiltration of

lamina propria T lymphocytes (LPLs) that we previously demonstrated to display a deficiency in branched N-glycosylation catalyzed by GnT-V(16). In this study we demonstrated that the simple glycan N-acetylglucosamine (GlcNAc) is able to repair the abovementioned deficiency having an important impact on the control of T cell-mediated immune response. The *ex vivo* supplementation of GlcNAc in T cells (purified from colonic mucosa of active UC patients) induces suppression of T cell proliferation, increased susceptibility to T cell apoptosis, inhibition of Th1/Th17-type inflammatory response, and suppression of T cell signaling and activation. Specifically, we found that GlcNAc supplementation resulted in T cell surface glycans remodeling characterized by an enhancement of the expression of branched N-glycans on the TCR that can be further extended with polylactosamine residues (ligand for galectins) and known to prevent TCR clustering and activation. These poly-LacNAc structures can be terminal sialylated. This modulation of the glycophenotype of T cells was shown to be translated in important regulatory effects on the adaptive immune response by hampering T cell function and activation, suppressing the release of potent pro-inflammatory cytokines known to promote the disease.

Taken together, metabolic enhancement of branched glycosylation on T cells, revealed to have immunomodulatory effects in UC with clinical relevance, paving the way to further explore the clinical applicability of this novel immunomodulatory agent in UC patients.

Table S1.

Fluorochrome	Antibody name	Source	Clone	Specificity
PerCP	CD4	BD Bioscience	clone SK3	anti-human
PE	CD8	BD Bioscience	clone SK1	anti-human
eF450	CD4	eBioscience	clone RPA-T4	anti-human
BV510	CD45	eBioscience	clone HI30	anti-human
Alexa Fluor488	Gata3	eBioscience	clone,TWAJ	anti-human
APC	RorγT	eBioscience	clone AFKJS-9	anti-human/mouse
PerCP-Cyanine 5.5	T-bet	eBioscience	clone eBio4B10	anti-human/mouse
PE	FoxP3	eBioscience	clone PCH101	anti-human/mouse
PerCP Cy 5.5	CD4	Biolegend	clone RPA-T4	anti-human
AF488	TNF-α	eBioscience	clone MAb11	anti-human
APC	IFN-γ	eBioscience	clone 4S.B3	anti-human
APC-eFluor® 780	Fixable Viability Dye	eBioscience		

The table summarizes the list of antibodies used for staining by flow cytometry experiments